Optimal combined proton-photon therapy schemes based on the standard BED model

ten Eikelder, S.C.M.; Den Hertog, D.; Bortfeld, T.; Perkó, Z.

DOI
10.1088/1361-6560/aafe52

Publication date
2019

Document Version
Final published version

Published in
Physics in Medicine and Biology

PAPER

Optimal combined proton–photon therapy schemes based on the standard BED model

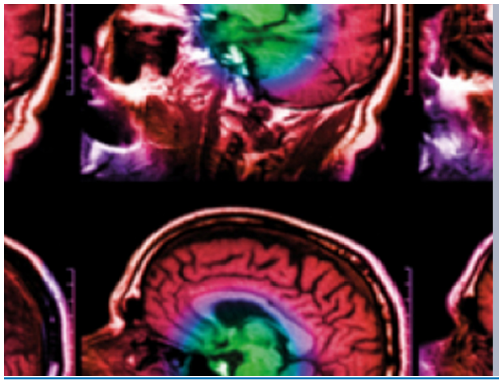

IOP Publishing Phys. Med. Biol. 64 (2019) 065011 (21pp) https://doi.org/10.1088/1361-6560/aafe52

Physics in Medicine & Biology

IPEM Institute of Physics and Engineering in Medicine

PAPER

RECEIVED
14 June 2018

REVISED
8 January 2019

ACCEPTED FOR PUBLICATION
14 January 2019

PUBLISHED
11 March 2019

Optimal combined proton–photon therapy schemes based on the standard BED model

S C M ten Eikelder[1,4], D den Hertog[1], T Bortfeld[2] and Z Perkó[2,3]

[1] Department of Econometrics and Operations Research, Tilburg University, Tilburg, The Netherlands
[2] Department of Radiation Oncology, Massachusetts General Hospital and Harvard Medical School, Boston, MA, United States of America
[3] Department of Radiation Science and Technology, Delft University of Technology, Delft, The Netherlands
[4] Author to whom any correspondence should be addressed.

E-mail: s.c.m.teneikelder@tilburguniversity.edu

Keywords: proton therapy, intensity-modulated radiation therapy (IMRT), optimization, multi-modality treatment, biologically effective dose (BED)

Supplementary material for this article is available online

Abstract

This paper investigates the potential of combined proton–photon therapy schemes in radiation oncology, with a special emphasis on fractionation. Several combined modality models, with and without fractionation, are discussed, and conditions under which combined modality treatments are of added value are demonstrated analytically and numerically. The combined modality optimal fractionation problem with multiple normal tissues is formulated based on the biologically effective dose (BED) model and tested on real patient data. Results indicate that for several patients a combined modality treatment gives better results in terms of biological dose (up to 14.8% improvement) than single modality proton treatments. For several other patients, a combined modality treatment is found that offers an alternative to the optimal single modality proton treatment, being only marginally worse but using significantly fewer proton fractions, putting less pressure on the limited availability of proton slots. Overall, these results indicate that combined modality treatments can be a viable option, which is expected to become more important as proton therapy centers are spreading but the proton therapy price tag remains high.

1. Introduction

In external beam radiation therapy (EBRT), the goal is to kill the tumor cells using ionizing radiation, while sparing the normal (healthy) tissues as much as possible. In spatial optimization, the radiation beam directions and intensities are optimized such that the dose to the healthy tissues is minimal, while still delivering the prescribed dose to the tumor. On the other hand, temporal optimization aims to select the optimal number of fractions of the treatment. The concept of fractionation is based on the observation that healthy cells have the capability to tolerate a larger dose if it is delivered in smaller fractions over multiple days, since they can repair radiation damage between treatments (Withers 1985, Fowler 1989).

Regarding the spatial component, different beam types (modalities) have different healthy tissue sparing properties. The relevant modalities for this work are photon beams (x-rays) and proton beams. Photon therapy is a conventional method that is by far the most frequently used. Proton therapy is a more advanced method, which theoretically has superior healthy tissue sparing properties, but is more expensive. While protons can offer higher dose conformity due to the pronounced Bragg peak, in the current planning approach often larger margins are used for protons than for photons due to range uncertainties (Perkó *et al* 2018). This is not a fundamental characteristic of proton therapy, but rather a consequence of limited image guidance and range control abilities in current proton therapy practice. Therefore, in present clinical setting using protons is not necessarily better for organs very close to the target (Perkó *et al* 2018), and investigating combined proton–photon treatments can be of interest.

In the fractionation optimization literature we can distinguish between single and multiple normal tissues, and between single and combined modality models. The biological effective dose (BED) model (Fowler 1989, 2010) has been the basis of most work on the topic. For the case with a single normal tissue and a single treatment modality, many numerical and analytical results have been derived. Mizuta *et al* (2012) mathematically prove that in this case the decision between hypofractionation and hyperfractionation depends on the ratio between the normal tissue α/β-ratio and the tumor α/β-ratio, where the α/β-ratio is a tissue-specific parameter representing the sensitivity of the tissue to fractionation. In the work of Unkelbach *et al* (2013a) this is generalized to the case where a spatially heterogeneous dose distribution is allowed via the introduction of dose sparing factors. Bortfeld *et al* (2015) further extend this model by including a tumor repopulation term. Many other studies examine specific aspects of the problem, or applications to specific tumor sites (Wein *et al* 2000, Yang and Xing 2005, Bertuzzi *et al* 2013).

Recently there has been significant progress on the optimal fractionation problem with a single treatment modality and multiple normal tissues. Saberian *et al* (2015) and Badri *et al* (2016) independently formulate and solve the optimization problem via a reformulation to a two variable linear programming problem. Saberian *et al* (2016) derive several results for the general optimization problem with maximum point dose, mean dose and dose-volume histogram (DVH) constraints. Amongst others they derive sufficient conditions for optimality of equal-dosage (more than one fraction) or single-dosage solutions. Kim *et al* (2015) apply the single modality optimal fractionation model with multiple normal tissues to phantom lung cases and find that, especially for cases with favorable geometry, nonconventional fractionation schemes may improve local tumor control while yielding shorter treatment courses. Perkó *et al* (2016) apply the same method to liver patients cases, and it is demonstrated that an intermediate fractionation scheme is optimal in the case of competing normal tissues.

In Unkelbach *et al* (2013b) and Unkelbach and Papp (2015) the spatiotemporal optimization problem is considered, where they simultaneously optimized the spatial dose distribution and the fractionation, in order to minimize a weighted sum of normal tissue doses and deviations from a prescribed tumor BED. Saberian *et al* (2017) consider the spatiotemporal optimal fractionation problem where they maximize tumor BED subject to BED constraints on multiple normal tissues. O'Connor *et al* (2018) solve the physical dose-based beam orientation optimization problem, allowing for different (non-coplanar) beam angles in different fractions.

Nill (2001, chapter 4) concludes that combined proton-photon treatments do not improve over proton treatments. However, they do not take into account fractionation. An application of the BED model to combined modality treatments is discussed in Bodey *et al* (2004), but this study combines photon therapy with targeted radionuclide therapy (a form of internal radiation therapy), instead of another EBRT modality.

This paper investigates combined modality fractionated treatments where each fraction employs either photon or proton therapy. Our three main contributions are as follows:

- **Analytical and numerical demonstration of optimal combined modality treatments:** We formulate and solve simplified combined modality optimization problems, that prove they can outperform single modality proton treatments for two reasons. First, in situations with multiple constraints, one constraint may be more restrictive for one treatment modality, while the other more restrictive for the other modality, making combined treatments optimal. Second, in situations where proton plans are superior in terms of dose, using photon fractions can yield plans that are better in terms of BED, due to the fractionation effect.
- **Demonstration of improved patient treatment plans:** We formulate the multiple normal tissue combined proton-photon fractionation optimization problem and solve it using real data from 17 patients, showing that for five combined modality treatments are an improvement over single modality proton treatments.
- **Demonstration of better resource allocation:** For three patients we show that a combined modality treatment plan can be found that is only marginally worse than the optimal proton treatment, while it uses fewer proton fractions.

The literature on (fractionation) optimization for combined proton-photon treatments is limited. The recent paper Unkelbach *et al* (2018) studies a similar combined modality problem, using spatiotemporal optimization. In their paper, first a 30-fraction plan is optimized for photons only and protons only. They use these to generate a reference plan, which is a proportional combination of these single modality plans such that the total number of photon and proton fractions is 30. Finally they optimize the combined modality plan, restricted to 30 fractions and enforcing that several performance measures do not deteriorate with respect to the reference plan. Unlike their approach, our method does not fix the total number of fractions and within a single modality we allow for nonuniform fractionation. Furthermore, while the method of Unkelbach *et al* (2018) is demonstrated only for a single patient, our larger data set indicates that several types of patients can be distinguished with regard to the benefit of combined modality. Lastly, we provide theoretical results that demonstrate the conditions under which combined modality can outperform single modality treatments.

Nourollahi *et al* (2018) also study BED-based combined modality fractionation optimization problems. However, they do not allow for a heterogeneous dose distribution via voxel-specific dose sparing factors, and consequently do not take DVH constraints into account either. Their approach and numerical results mainly focus on hypothetical cases with a single healthy tissue, whereas we find that one of the reasons for optimality of combined modality treatments is the interplay of multiple healthy tissues.

The outline of this paper is as follows. Section 2.1 discusses two reasons why combined proton–photon treatments may outperform single modality treatments. Section 2.2 presents the full combined proton-photon fractionation optimization problem. In section 3 this model is tested on a data set of liver patients treated at Massachusetts General Hospital (MGH) and the results are presented. Section 4 discusses the results and their relevance to clinical practice. Last, section 5 presents our conclusions.

2. Methods and materials

Our approach is based on the standard biological effective dose (BED) model. Tumor repopulation is not taken into account. The standard BED model states that the biological effect of a dose D given to a tissue in N fractions is given by

$$\text{BED} = D(1 + \frac{1}{\alpha/\beta}\frac{D}{N}), \tag{1}$$

where α/β is a parameter indicating the fractionation sensitivity of the tissue, and BED is measured in $\text{Gy}_{\alpha/\beta}$ instead of Gy. We generalize BED equation (1) to the situation with unequal dose per fraction and two treatment modalities. Due to additivity, the BED to an irradiated tissue equals the BED from a photon dose plus the BED from a proton dose. Let $D_i^T = \sum_{t_i=1}^{N_i} d_{i,t_i}$ be the total dose to the tumor of modality i, where d_{i,t_i} is the dose of modality i to the tumor in fraction t_i, and N_i is the number of fractions of modality i. Subscripts $i = \gamma$ and $i = p$ stand for photons and protons, respectively. Let $s_{i,j}$ denote the dose sparing factor of any voxel j in the tumor or in an OAR for treatment modality i. The BED to voxel j is given by

$$\text{BED}_j = \sum_{t_\gamma=1}^{N_\gamma} s_{\gamma,j} d_{\gamma,t_\gamma} + \rho \sum_{t_\gamma=1}^{N_\gamma} s_{\gamma,j}^2 d_{\gamma,t_\gamma}^2 + \sum_{t_p=1}^{N_p} s_{p,j} d_{p,t_p} + \rho \sum_{t_p=1}^{N_p} s_{p,j}^2 d_{p,t_p}^2, \tag{2}$$

where ρ denotes the inverse α/β ratio of the tissue containing voxel j.

In section 2.1 we describe two reasons why combined proton–photon treatments may outperform single modality treatments. Section 2.2 presents the BED-based full combined proton-photon fractionation optimization problem.

2.1. Two reasons why combined proton-photon treatments can outperform single modality treatments

We consider a situation with two organs-at-risk (OARs). OAR 1 includes the tumor and OAR 2 is another organ close to the tumor, see figure 1. The outer circle indicates OAR 1, the tumor is the black circle in the middle, and the blue circle indicates OAR 2. No other OARs play a significant role. Figure 1 is naturally a 2D representation of a 3D situation, with OAR 2 interpreted as an organ close to the tumor.

For the photon dose distribution (figure 1(a)) we assume that the gantry completes a full rotation around the patient shooting beams from all angles. These angles intersect in the area within the red circle, where the dose is high. Outside this area, we assume that photon beams do not intersect, so the dose is equally low everywhere (green area). Thus, the tumor and a small part of OAR 1 receive a uniform high dose, and the rest of OAR 1 and the entire volume of OAR 2 (blue area) receive a uniform low dose.

For the proton dose distribution (figure 1(b)) there is a single beam. There is a high dose area (spread out Bragg Peak in red) and a low dose area (the beam entrance in green). Thus, the tumor, part of OAR 1 (around the tumor) and part of OAR 2 (intersection of red and blue area) receive a uniform high dose, part of OAR 1 receives a uniform low dose, and the remaining parts of OAR 1 and OAR 2 receive no dose.

We need to determine how much dose should be given with each modality, i.e. how much the dose distributions described above should be scaled. The corresponding optimization problem can be formulated in terms of dose, or in terms of BED. In the latter case, it must also be determined how many fractions are needed for each modality. The objective is to maximize the dose or BED to the tumor, such that the dose or BED to the OARs remains below some tolerance level. If the optimal solution makes use of both photon and proton dose (and fractions), this implies that combined modality yields a better solution than single modality, and analyzing the underlying mathematical model can reveal the conditions under which this occurs. In sections 2.1.1 and 2.1.2 we identify two such reasons. Combined modality treatments can also be shown to be optimal (see appendix A.3) if one minimizes the dose or BED to one of the OARs, while one constrains the tumor dose or BED to a prescribed level and the dose or BED to the other OAR below a tolerance.

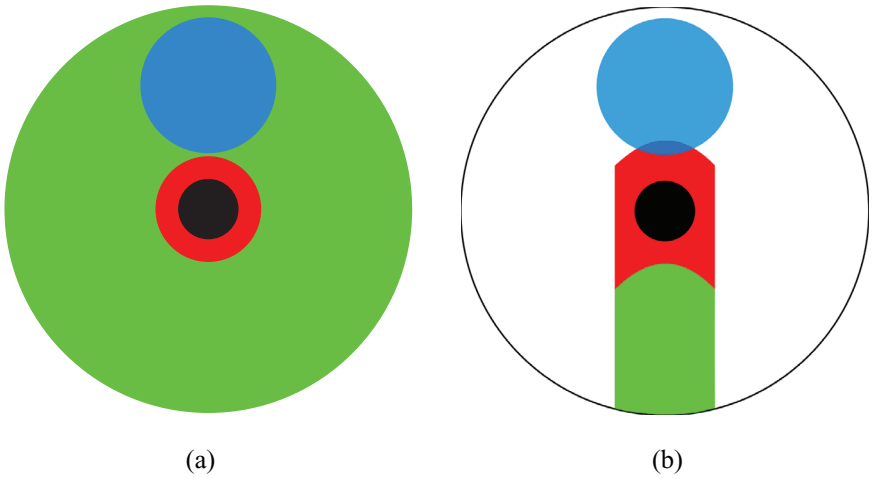

Figure 1. Schematic view of the simplified (2D) scenario with an OAR containing a tumor, and a second nearby OAR. The outer circle represents OAR 1 with the tumor in the middle (black), and the blue circle represents OAR 2. (a) The photon dose distribution causes 'high' damage inside the intersection of the beams (red) and 'low' damage everywhere else (green). (b) The proton beam causes 'high' damage in the spread out Bragg Peak (red), 'low' damage at the entrance (green) and no damage anywhere else.

2.1.1. Optimality due to competing constraints, with protons and photons being better for different ones

The first reason why combined modality treatments may outperform single modality proton treatments is due to the different shape of the high dose regions of the photon and proton dose distributions, when there are multiple OARs in proximity to the tumor. As seen in figure 1, part of OAR 2 falls in the proton high dose region, but not in the photon high dose region, meaning that a DVH or maximum point dose constraint may be more restrictive for protons than for photons. For example, consider a DVH constraint on OAR 2 where the restricted volume (the maximum volume for which the dose may exceed a given tolerance level) is smaller than the high dose region of OAR 2 for the proton dose distribution. This constraint is much more restrictive for protons than for photons. Hence, if we only set this constraint, the photon dose distribution is favorable. On the other hand, a mean dose constraint on OAR 1 is more restrictive for the photon dose distribution than for the proton dose distribution, due to the much larger photon low dose region. Hence, a mean dose constraint favors protons.

In essence, we have two competing constraints, both favoring a different treatment modality. A combined modality treatment that uses part photons and part protons is able to balance these two interests best. As mathematically derived in appendix A.1, a combined modality treatment can deliver a higher dose to the tumor than either modality alone, while it also satisfies the DVH and mean dose constraints on OAR 2 and OAR 1 respectively.

A similar conclusion can be reached if a DVH constraint is set such that the proton entrance dose is constrained, or if more DVH constraints are added, and the example can naturally be generalized to allow more proton beams. While we supposed a larger high dose region for protons than for photons, this is not a necessary condition for our statements to hold, simple shape differences can also lead to similar conclusions (protons depositing high dose in OAR 2 while photons not). Moreover, proton plans in practice can indeed show larger high dose regions compared to photon plans due to larger planning margins (due to more uncertainty in range, e.g. for organs with significant internal motion) and worse lateral penumbra (Perkó *et al* 2018). As shown in section 3, this is truly the case for our patient data.

2.1.2. Optimality due to having more fractions, even if photons are somewhat worse

The second reason why combined modality may outperform single modality proton treatments is related to the fractionation effect. If the α/β-ratio of the OAR is smaller than that of the tumor, the benefit of fractionation is larger for the OAR than for the tumor. For simplicity, suppose the α/β-ratio of the tumor is sufficiently large so that we can neglect the fractionation effect and optimize for maximum tumor physical dose. Next, consider a mean dose constraint on OAR 1. For a fixed dose to (part of) OAR 1, the BED to (that part of) OAR 1 will be lower if this dose is administered over multiple fractions. As the number of fractions does not influence the damage to the tumor, once we are delivering a non-zero dose with a modality (photons or protons), it will always be optimal to use the maximum number of allowed fractions for this modality.

For the same tumor dose, the proton dose distribution has a lower mean dose in OAR 1 than the photon dose distribution. Therefore, when using equal dose per fraction to minimize BED, protons also deliver lower mean BED in OAR 1 than photons for a given number of fractions, and it is always optimal to set a non-zero dose per fraction to the proton fractions. In case we use only protons, the proton dose per fraction is increased until we

reach the mean BED tolerance on OAR 1. Delivering part of the dose via photon fractions allows for a lower dose per fraction in the proton fractions. Adding these photon fractions naturally leads to slightly worse OAR sparing in terms of physical dose, however due to the higher total number of fractions, the BED in OAR 1 does not necessarily increase. Whether or not using the photon fractions is optimal depends on the trade-off between the worse OAR sparing in terms of physical dose and the benefit of fractionation. In appendix A.2 we demonstrate that this trade-off indeed occurs, and that combined proton–photon treatments outperform single modality proton treatments in terms of achievable tumor dose, if the BED tolerance level exceeds a threshold. That is, unless the BED tolerance of OAR 1 is very restrictive, the benefit of having more fractions outweighs the disadvantage of some of these fractions (the photon fractions) having worse physical OAR sparing.

2.2. General combined modality fractionation model with multiple OARs

In this section the general optimization problem for the combined proton-photon optimal fractionation problem with multiple normal tissues is formulated. The model can take into account maximum point dose, mean dose and dose-volume constraints, accepts arbitrary proton and photon dose distributions as given inputs, and determines the optimal dose for each modality (i.e. how much the dose distributions need to be scaled) and the number of fractions these doses should be delivered. Note that the general model described in this section is completely separate from the simplified geometry of section 2.1 and makes no assumptions regarding the dose distributions.

Similar to the approach of Saberian *et al* (2015) for the single modality fractionation problem, we formulate our model not in terms of dose vectors d_γ and d_p (for photons and protons respectively), but instead in terms of four new variables. For photons, let x_γ and y_γ denote the total dose and the sum of squared doses. For protons, denote these quantities by x_p and y_p, respectively. Thus, we use the following substitutions:

$$x_\gamma = \sum_{t_\gamma=1}^{N_\gamma} d_{\gamma,t_\gamma},\ y_\gamma = \sum_{t_\gamma=1}^{N_\gamma} d_{\gamma,t_\gamma}^2,\ x_p = \sum_{t_p=1}^{N_p} d_{p,t_p},\ y_p = \sum_{t_p=1}^{N_p} d_{p,t_p}^2. \tag{3}$$

First we consider the objective function. Let n^T be the number of voxels in the tumor, and ρ^T the inverse α/β-ratio of the tumor. Let $s_{i,j}^T$ be the dose sparing factor of tumor voxel j for treatment modality i. The objective is to maximize the mean target BED, which can be formulated as

$$\max_{x_\gamma,y_\gamma,x_p,y_p} \frac{1}{n^T}\sum_{j=1}^{n^T}\left(s_{\gamma,j}^T x_\gamma + \rho^T (s_{\gamma,j}^T)^2 y_\gamma + s_{p,j}^T x_p + \rho^T (s_{p,j}^T)^2 y_p\right). \tag{4}$$

Next, we consider the constraint types. Let $\mathcal{M}_1$, $\mathcal{M}_2$ and $\mathcal{M}_3$ denote the set of maximum point dose, DVH and mean dose constraints, respectively. For the OAR corresponding to constraint m, let n^m denote the number of voxels in the OAR, ρ^m denote the inverse α/β ratio for the OAR, and $s_{i,j}^m$ be the dose sparing factor of voxel j in the OAR for treatment modality i.

2.2.1. Maximum point dose constraints

A maximum point dose constraint on OAR m states that no voxel in the OAR may receive a dose higher than dose $D_{\max}^m$ if delivered in N^m fractions. This tolerance dose corresponds with a BED of

$$\mathrm{BED}_{\max}^m = D_{\max}^m\left(1 + \rho^m \frac{D_{\max}^m}{N^m}\right). \tag{5}$$

Thus, the constraint reads

$$s_{\gamma,j}^m x_\gamma + \rho^m (s_{\gamma,j}^m)^2 y_\gamma + s_{p,j}^m x_p + \rho^m (s_{p,j}^m)^2 y_p \leqslant \mathrm{BED}_{\max}^m,\ \forall j = 1,\dots,n^m,\ m \in \mathcal{M}_1. \tag{6}$$

2.2.2. DVH constraints

For a DVH constraint on OAR m, no more than a fraction F^m of the OAR volume V^m may receive a dose higher than D_{dvh}^m if given in N^m fractions. This tolerance is equivalent to a BED of

$$\mathrm{BED}_{\mathrm{dvh}}^m = D_{\mathrm{dvh}}^m\left(1 + \rho^m \frac{D_{\mathrm{dvh}}^m}{N^m}\right). \tag{7}$$

The constraint now reads

$$\begin{aligned} s_{\gamma,j}^m x_\gamma + \rho^m (s_{\gamma,j}^m)^2 y_\gamma + s_{p,j}^m x_p + \rho^m (s_{p,j}^m)^2 y_p \leqslant \mathrm{BED}_{\mathrm{dvh}}^m + M(1-u_j^m),\\ \forall j = 1,\dots,n^m,\ m \in \mathcal{M}_2, \end{aligned} \tag{8}$$

where $M \in \mathbb{R}$ is a sufficiently large positive number, and u_j^m are binary decision variables for $\forall j = 1,\dots,n^m$. Let u denote the stacked vector of all binary variables for $\forall m \in \mathcal{M}_2$. A value $u_j^m = 1$ implies that voxel j in the

OAR corresponding to constraint m receives a BED lower than or equal to $\text{BED}^m_{\text{dvh}}$ and $u^m_j = 0$ implies that voxel j receives a BED higher than $\text{BED}^m_{\text{dvh}}$. Because volume V^m is discretized into n^m voxels, we add extra constraints that at least $n^m - \lfloor F^m n^m \rfloor$ voxels must receive a BED lower than $\text{BED}^m_{\text{dvh}}$:

$$\sum_{j=1}^{n^m} u^m_j \geqslant n^m - \lfloor F^m n^m \rfloor, \quad \forall m \in \mathcal{M}_2, \tag{9}$$

$$u^m_j \in \{0,1\}, \ \forall j \in \mathcal{N}^m, \ \forall m \in \mathcal{M}_2. \tag{10}$$

2.2.3. Mean dose constraints

A mean dose constraint on OAR m states that a mean dose of D^m_{mean} over all voxels is tolerated if given in N^m fractions. This constraint can be formulated as

$$\frac{1}{n^m}\sum_{j=1}^{n^m}\left(s^m_{\gamma,j}x_\gamma + \rho^m(s^m_{\gamma,j})^2 y_\gamma + s^m_{p,j}x_p + \rho^m(s^m_{p,j})^2 y_p\right) \leqslant \text{BED}^m_{\text{mean}}. \tag{11}$$

For the mean dose tolerance, we note that there is a difference between the BED of the mean dose and the mean BED, due to the influence of the spatial distribution of the dose. In Perkó *et al* (2018) this effect is captured for a single modality by a parameter named the dose shape factor. The dose shape factor φ^m for the photon dose distribution in the OAR corresponding to constraint m is given by

$$\varphi^m = \frac{n^m \sum_{j=1}^{n^m} s^2_{\gamma,j}}{\left(\sum_{j=1}^{n^m} s_{\gamma,j}\right)^2}, \tag{12}$$

and similar for the proton dose distribution. For more details, see Perkó *et al* (2018).

2.2.4. Final optimization problem

All put together, the optimization problem reads:

$$\max_{x_\gamma, y_\gamma, x_p, y_p, u} \quad \frac{1}{n^T}\sum_{j=1}^{n^T}\left(s^T_{\gamma,j}x_\gamma + \rho^T(s^T_{\gamma,j})^2 y + s^T_{p,j}x_p + \rho^T(s^T_{p,j})^2 y_p\right), \tag{13a}$$

s.t.
$$s^m_{\gamma,j}x_\gamma + \rho^m(s^m_{\gamma,j})^2 y_\gamma + s^m_{p,j}x_p + \rho^m(s^m_{p,j})^2 y_p \leqslant \text{BED}^m_{\text{max}}, \quad \forall j = 1,\ldots,n^m, \ \forall m \in \mathcal{M}_1, \tag{13b}$$

$$s^m_{\gamma,j}x_\gamma + \rho^m(s^m_{\gamma,j})^2 y_\gamma + s^m_{p,j}x_p + \rho^m(s^m_{p,j})^2 y_p \leqslant \text{BED}^m_{\text{dvh}} + M(1-u^m_j), \quad \forall j = 1,\ldots,n^m, \ \forall m \in \mathcal{M}_2, \tag{13c}$$

$$\sum_{j=1}^{n^m} u^m_j \geqslant n^m - \lfloor F^m n^m \rfloor, \quad \forall m \in \mathcal{M}_2, \tag{13d}$$

$$u^m_j \in \{0,1\}, \ \forall j = 1,\ldots,n^m, \ \forall m \in \mathcal{M}_2, \tag{13e}$$

$$\frac{1}{n^m}\sum_{j=1}^{n^m}\left(s^m_{\gamma,j}x_\gamma + \rho^m(s^m_{\gamma,j})^2 y_\gamma + s^m_{p,j}x_p + \rho^m(s^m_{p,j})^2 y_p\right) \leqslant \text{BED}^m_{\text{mean}}, \quad \forall m \in \mathcal{M}_3, \tag{13f}$$

$$\sqrt{y_\gamma} \leqslant x_\gamma \leqslant \sqrt{N_\gamma y_\gamma}, \tag{13g}$$

$$\sqrt{y_p} \leqslant x_p \leqslant \sqrt{N_p y_p}, \tag{13h}$$

$$x_\gamma \geqslant 0, \ y_\gamma \geqslant 0, \ x_p \geqslant 0, \ y_p \geqslant 0. \tag{13i}$$

Constraints (13*g*) and (13*h*) model the relations between decision variables x_γ and y_γ, and x_p and y_p, respectively. In the supplementary material (section D, suppl. (stacks.iop.org/PMB/64/065011/mmedia)) it is shown that (13) is equivalent to (D.9), i.e. the optimization problem in terms of the original dose-per-fraction vectors $d_\gamma \in \mathbb{R}^{N_\gamma}_+$ and $d_p \in \mathbb{R}^{N_p}_+$. Compared to the single modality model in Saberian *et al* (2015) (also detailed in appendix B), the main difficulty is found in the DVH constraints, as there is no a-priori ordering of the voxels in terms of BED. To overcome this we developed the algorithm described in section 2.2.5.

2.2.5. Optimization algorithm

To solve problem (13) we make use of the following variable transformation:

$$\theta = \frac{x_\gamma}{x_\gamma + x_p}, \quad v_\gamma = \frac{x_\gamma^2}{y_\gamma}, \quad v_p = \frac{x_p^2}{y_p}. \tag{14}$$

Variable θ can be interpreted as the fraction of photon dose to total dose. Variables v_γ and v_p are, when rounded up, equal to the number of used photon and proton fractions, respectively. The new set of variables is $\{x_\gamma, u, \theta, v_\gamma, v_p\}$. Let f and $\mathcal{F}$ denote the objective function and feasible set of (13) in terms of the new variable set.

We split the new variables set into two sets: $\{x_\gamma, u\}$ and $\{\theta, v_\gamma, v_p\}$. In the supplementary material (section E.1, suppl.) it is described how for fixed variables $\{\theta, v_\gamma, v_p\}$ we can (exactly) compute the optimal values of $\{x_\gamma, u\}$. The described procedure eliminates the (large number of) binary variables u and requires only a sorting algorithm to compute the optimal value for x_γ. Hence, this procedure is very fast. Denote these optimal values by $x_\gamma^*(\theta, v_\gamma, v_p)$ and $u^*(\theta, v_\gamma, v_p)$. Then we can concisely represent problem (13) as

$$\max_{\theta, v_\gamma, v_p} \; f(x_\gamma^*(\theta, v_\gamma, v_p), u^*(\theta, v_\gamma, v_p), \theta, v_\gamma, v_p) \tag{15a}$$

$$\text{s.t.} \quad \{x_\gamma^*(\theta, v_\gamma, v_p), u^*(\theta, v_\gamma, v_p), \theta, v_\gamma, v_p\} \in \mathcal{F}, \tag{15b}$$

which is a problem of only three variables, as (θ, v_γ, v_p) are all scalar variables. We solve (15) via a generalized pattern search (GPS) algorithm (Audet and Dennis 2003). GPS is an optimization algorithm that does not require a gradient, nor does it require the objective function to be continuous. To improve performance, we take a multi-start approach, details of which are provided in the supplementary material (section E.2, suppl.).

This separation into two variable sets also enables setting an additional constraint on the dose per fraction values. Specifically, it allows us to set a minimum dose per fraction value $d_{\min}$ and a maximum dose per fraction value $d_{\max}$. This may be clinically interesting, as it avoids treatments that could be considered unrealistic in current practice, with too high or negligibly small dose per fraction values.

2.2.6. Implementation

All computations were performed on a 2.6 GHz Intel-Core i5 PC with 8 GB RAM, using the software package MATLAB R2017b (Mathworks, Natick, MA, US). The MATLAB toolbox CERR (Computation Environment for Radiotherapy Research, Deasy *et al* (2003)) is used to visualize and analyze patient data, and to transfer the data to the MATLAB environment. For all patients we solve problem (13) using the MATLAB function `patternsearch` for all combinations of N_γ and N_p such that $N_\gamma + N_p = 15$, so the total number of allowed fractions is 15. The single modality proton optimal fractionation problem (see appendix B) is also solved. During the optimization procedure, we set a minimum and a maximum dose per fraction of $d_{\min} = 1$ Gy fx^{-1} and $d_{\max} = 10$ Gy fx^{-1}, respectively.

2.2.7. Patient data

The data set is a subset of the data set used in Perkó *et al* (2018), consisting of actual patient data (in DICOM format) from 17 patients who were treated at Massachusetts General Hospital, and was provided by physicians collaborating with the physics research group. All patients in the data set are liver patients and were treated with passively scattered protons in practice, in 5 or 15 fractions. All proton plans incorporated compensator smearing and are adjusted for relative biological effectiveness (RBE) by setting $\text{RBE}_{\text{proton}} = 1.1$. Next to the clinically used proton plans, the treatment planners also derived photon plans for these patients, taking into account all proper clinical measures to deal with uncertainties. For more details on patient selection and how uncertainties were handled we refer to Perkó *et al* (2018).

Patients with liver tumors are interesting for combined modality treatments, due to the large number of neighbouring healthy tissues, and the different constraints on the tissues that are in the paths of the beams. Our patient cohort well reflected that proton distributions are not necessarily superior in terms of the high dose area: due to larger motion uncertainty they typically used larger margins. Although the used proton plans are passive scattering plans, even in IMPT larger margins could be present than in their photon counterparts.

3. Results for patients for combined modality fractionation model with multiple OARs

The objective is to maximize the BED to the gross target volume (GTV). Throughout the results and discussion the terms GTV and tumor are used interchangeably. Table 1 presents the most important constraints for all patients in terms of dose and BED. In clinical practice, the dose tolerance levels for healthy liver mean dose are not hard constraints but are used as 'goals', meaning that for a given number of fractions a range of dose tolerances is acceptable. Correspondingly, in our optimization dose tolerance values are picked such that the resulting GTV

Table 1. Most important constraints for the patients in the numerical study. DVH constraints are formulated either in the largest volume (in *cc* or %) that may be violated or in the smallest volume that needs to be spared. Our cases did not have any maximum point dose constraints.

Constraints			
OAR	Dose tolerance (Gy)	Fractions	Constraint type
Liver-CTV	15	5	DVH: sparing $> 700cc$
	10	5	DVH: sparing $> 30\%$
	[8, 17]	5	Mean dose (goal range)
	[16, 27]	15	Mean dose (goal range)
Stomach	{30, 40}	{5, 15}	DVH: violation $< 0.5cc$
	{25, 36}	{5, 15}	DVH: violation $< 5cc$
Duodenum	{30, 40}	{5, 15}	DVH: violation $< 0.5cc$
	{25, 36}	{5, 15}	DVH: violation $< 5cc$
Small bowel	{30, 40}	{5, 15}	DVH: violation $< 0.5cc$
	{25, 36}	{5, 15}	DVH: violation $< 5cc$
Large bowel	{32, 40}	{5, 15}	DVH: violation $< 0.5cc$
Cord	{25, 37.5}	{5, 15}	DVH: violation $< 0.5cc$

BED is between 50 and 200 Gy. This value is applied consistently in the optimization of the single modality photon and proton treatments and the combined modality treatment, to allow for a fair comparison. In clinical practice, the range of dose tolerances for the 5 and 15 fraction regimens are [13 Gy, 17 Gy] and [23 Gy, 27 Gy], respectively. However, for cases with very small tumors, the mean GTV BED can take very high values before these liver mean dose constraints are binding. Hence, we extend these dose tolerance ranges to [8 Gy, 17 Gy] for the five fraction regiment and [16 Gy, 27 Gy] for the 15 fraction regimen.

In clinical practice, the healthy liver (liver–clinical target volume (CTV)) constraints are either mean dose constraints or DVH constraints, where DVH constraints are used for cases with large tumors and mean dose constraints are used for cases with small tumors. In our numerical experiments we use both sets of constraints simultaneously, except that the 700*cc* healthy liver DVH constraint is omitted for those patients where it was violated clinically, to achieve an adequate tumor dose. Hence, for several cases more constraints are included than what was done clinically. We emphasize that for every patient, the same set of constraints is used for the single and combined modality optimization.

To compare the combined modality results to the single modality results, we determine the physical dose that is required in the single modality proton fractionation scheme to obtain the combined modality tumor BED. This physical dose value is named the *BED equivalent dose* of the combined modality treatment, and is used as a performance measure for a fractionation scheme.

Results indicate that the potential for combined modality solutions is quite substantial. Out of 17 patients, for five patients there is a combined modality treatment that offers an improvement over the optimal single modality proton treatments. This is discussed in section 3.1. For three patients a near-optimal combined modality solution exists that can reduce the number of required proton fractions; this is discussed in section 3.2. For the remaining nine patients combined modality treatments cannot offer any interesting alternative compared to the optimal single modality proton treatment, because the proton dose distribution is better than the photon dose distribution for all relevant OARs. This group is discussed in section 3.3.

3.1. Group 1: combined modality treatment offers clear improvement

For five patients, results indicate that a combined modality treatment can give better results than the single modality proton treatment. Figure 2 compares the optimal single modality proton treatment to the combined modality treatment that is found via solving (13). Above every bar the resulting BED equivalent physical tumor dose and the number of used fractions are reported as *(photon fx, proton fx)*.

For these five patients, the BED equivalent dose is between 7.2% and 14.8% higher in the combined modality treatment than in the single modality proton treatment. For patients P_2 and P_3 the combined modality optimum uses more proton fractions than the single modality proton optimum, but for the other three patients the number of used proton fractions is in fact lower. Typically, for these patients the two modalities have different binding constraints. That is, there are competing constraints, which prefer different treatment modalities. In a combined modality treatment both of these constraints are binding. This will be discussed in more detail in section 4.

As an additional analysis, we have made slight adaptations to the optimization model, and minimized the mean liver BED under the restriction that the mean tumor BED should be at least the mean tumor BED of the optimal single modality proton treatment. For existence of a combined modality treatment with lower mean liver BED than the optimal proton treatment, it is necessary for a patient to be in group 1 (in other groups com-

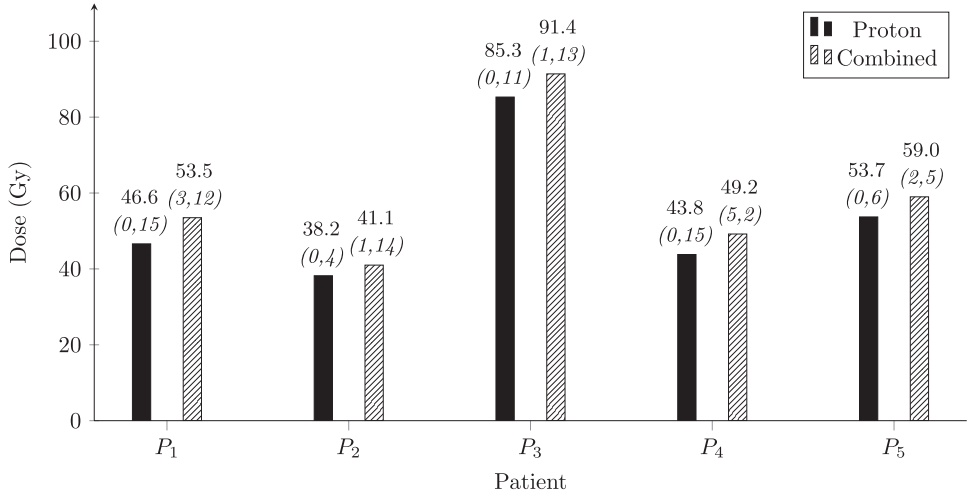

Figure 2. Results for group 1. Black bars indicate proton results, dashed bars indicate combined modality results. Reported doses are in BED equivalent physical dose, to correct for different fractionation schemes. Above every bar the resulting BED equivalent dose and the number of used fractions is reported as *(photon fx, proton fx)*.

bined modality cannot attain the required tumor BED), but this is not sufficient. More details on this are provided in sections 4.2 and 4.5. Out of the five patients in group 1, for two patients (P_2 and P_3) combined modality can reduce mean liver BED (decrease of 8.0% and 10.2% in BED equivalent dose, respectively).

3.2. Group 2: combined modality treatment offers alternative with fewer proton fractions

This group consists of three patients. For these patients the optimum is a single modality proton treatment. However, there are near-optimal combined modality solutions that use fewer proton fractions. If we force the use of a number of photon fractions in (13), we obtain alternative combined modality treatments. Figure 3 compares the optimal single modality proton treatment to an alternative combined modality treatment.

We emphasize that the reported combined modality treatments in figure 3 are an example of a combined modality treatment that is optimal if we force the use of a number of photon fractions (13), but this number may be varied. For example, for patient P_6 we forced the use of eight photon fractions, but a smaller number is also possible. This yields a BED equivalent GTV dose between that of the *(0,15)* and the *(8,7)* treatment.

For each of these patients several proton fractions can be replaced by photon fractions without a large decrease in average GTV BED equivalent dose. For example, for patient P_6 going from the *(0,15)* treatment to the *(8,7)* treatment gives a decrease of 1.4 Gy in BED equivalent dose, which is on average −0.175 Gy per replaced fraction. Such an alternative combined modality treatment is interesting if only a limited number of proton fractions is available, and these must be allocated among a set of patients.

3.3. Group 3: single modality proton therapy is superior

For the remaining nine patients, the proton plan is significantly better than the photon plan for all relevant OARs and a combined modality treatment is not very suitable. The optimal single modality proton treatments are reported in table 2. For most of these patients, it may only be optimal to combine proton fractions with photon fractions if the maximum number of proton fractions that can be allocated is very low. In that case, the added photon fractions provide the benefit of the fractionation effect. Typically, the dose distributions for these patients are such that there is only one OAR that restricts the dose that can be delivered, and the proton plan spares this OAR better than the photon plan. For illustration, columns 4 and 5 of table 2 give the optimal treatment if we force the use of at least one photon fraction. For some patients the deterioration in BED equivalent GTV dose is not very large. However, in all these cases only one photon fraction with a dose between 1.0 and 1.2 Gy (the lower bound is 1.0 Gy) is used. Hence, for these patients enforcing the use of a single photon fraction has a visible negative effect even if the photon fraction uses only a low dose.

4. Discussion

This section provides a detailed discussion of the results of sections 3.1 and 3.2, by analysing the results for two patients: patient P_1 (section 4.1) and P_6 (section 4.3). Additionally, section 4.2 discusses the results for OAR sparing.

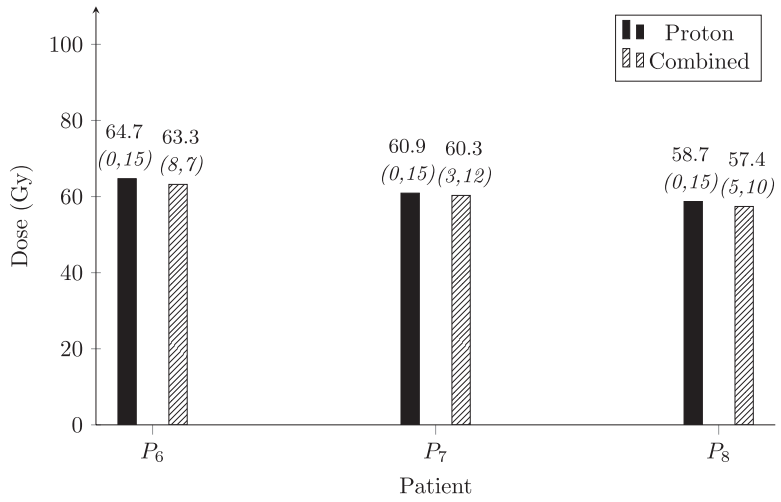

Figure 3. Results for group 2. Black bars indicate the optimal treatments (single modality proton), dashed bars indicate an example of a combined modality alternative treatment. Reported doses are in BED equivalent physical dose, to correct for different fractionation schemes. Above every bar the resulting BED equivalent dose and the number of used fractions is reported as *(photon fx, proton fx)*.

Table 2. Results for group 3. The optimal single modality proton solution is reported, with doses in BED equivalent dose. The reported combined modality alternatives are the optimal treatments if we force the use of at least one photon fraction. The used photon fraction in the combined modality solutions has a dose between 1.0 and 1.2 Gy for all patients. The number of used fractions is reported as *(photon fx, proton fx)*.

	Proton optimum		Combined modality alternative	
Patient	Dose (Gy)	Fractions	Dose (Gy)	Fractions
P_9	55.0	(0,15)	54.6	(1,14)
P_{10}	71.0	(0,15)	70.2	(1,14)
P_{11}	72.4	(0,15)	71.9	(1,14)
P_{12}	78.8	(0,15)	78.4	(1,14)
P_{13}	74.4	(0,15)	73.7	(1,14)
P_{14}	87.2	(0,9)	86.5	(1,9)
P_{15}	63.2	(0,15)	62.8	(1,14)
P_{16}	66.9	(0,15)	66.5	(1,14)
P_{17}	92.5	(0,15)	91.8	(1,14)

4.1. Illustration of group 1

Patient P_1 was clinically treated with 15 proton fractions. The location of the GTV in the liver is indicated in figure 4, which displays two CT slices for both the photon and the proton dose distribution. For the most relevant constraints see table 1. The clinical plan violated the 700*cc* constraint, hence it is omitted here as well.

For this patient the dose tolerances for the healthy liver mean constraints are 17 Gy in 5 fractions and 27 Gy in 15 fractions. Table 3 shows the results for the optimal combined modality treatment and the optimal single modality treatments. The optimal combined modality treatment delivers an average GTV BED of 72.5 Gy_{10}, and uses three photon fractions and 12 proton fraction. The corresponding BED equivalent GTV dose (in 15 fractions) is 53.5 Gy. The optimal single modality proton treatment delivers an average GTV BED of 61.0 Gy_{10} in 15 fractions; the corresponding BED equivalent dose is 46.6 Gy. Therefore, the combined modality treatment gives an improvement in BED equivalent dose of 14.8% compared to the optimal single modality proton treatment.

In the single modality proton case the 0.5*cc* duodenum DVH constraint is binding, and in the single modality photon case the (17 Gy in five fractions) liver-CTV mean dose constraint is binding (technically, the 30% liver-CTV DVH constraint is also binding). Note that single modality photon is the only treatment that has non-constant dose per fraction. The optimal single modality proton treatment has constant dose per fraction, and the optimal combined modality treatment has constant dose per fraction within each modality. Restricting the single modality photon case to constant dose per fraction as well, the optimal treatment delivers an average GTV BED of 60.9 Gy_{10}, using ten fractions of 4.3 Gy fx^{-1}. This is only marginally worse than the optimal non-constant dose per fraction single modality photon treatment.

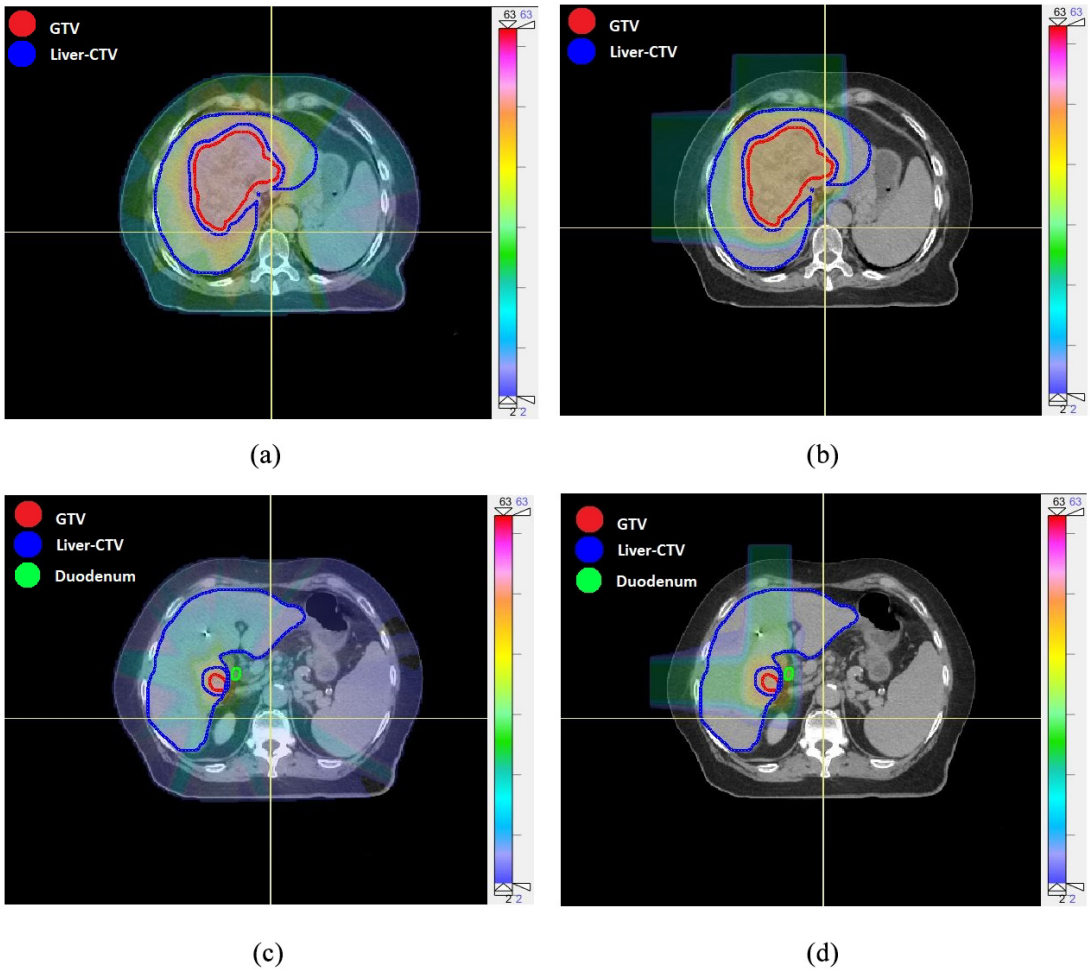

Figure 4. Spatial dose distribution in photon and proton plans of patient P_1 in two slices. The GTV, liver-CTV and duodenum are delineated. (a) Photon, CT slice 1. (b) Proton, CT slice 1. (c) Photon, CT slice 2. (d) Proton, CT slice 2.

Table 3. Results for patient P_1. The optimal combined modality treatment delivers a higher BED equivalent dose to the GTV than the single modality treatments. For this patient the optimal single modality photon and proton plans perform similarly.

	Single modality photon	Single modality proton	Combined modality
GTV BED	61.0 Gy_{10}	61.0 Gy_{10}	72.5 Gy_{10}
BED equivalent dose	46.5 Gy	46.6 Gy	53.5 Gy
Photon fractions	10 fx (4.2 Gy fx^{-1}) 1 fx (1.0 Gy fx^{-1})	—	3 fx (4.7 Gy fx^{-1})
Proton fractions	—	15 fx (3.1 Gy fx^{-1})	12 fx (3.2 Gy fx^{-1})

If both photon and proton fractions are used, the GTV BED can be increased (compared to the single modality cases) such that both the liver mean dose constraint and the duodenum constraint are binding, while the 30% liver-CTV DVH constraint is also satisfied.

As seen on the CT slices in figure 4(b), a small portion of the duodenum volume extends to the center of the high dose region of the proton beam. The photon dose to this area is much lower. The only way for protons to protect the duodenum is to keep the dose per fraction relatively low, consequently the dose per fraction in the single modality proton plan is only 3.1 Gy fx^{-1} (see table 3). In comparison, using photons allows mild hypofractionation, until the liver mean dose constraint becomes binding. The combined treatment allows us to deliver some of the proton dose using photons, which are less restrictive for the duodenum. Therefore, we can increase the GTV BED until the liver mean dose constraint also becomes binding. Essentially, some of the proton fractions are omitted to give a hypofractionated photon dose boost.

Figure 5 shows the DVH lines of the combined modality optimal solution and the single modality proton optimal solution for the GTV and some relevant OARs, in terms of BED equivalent physical dose in 15 fx. Clearly, the GTV dose is significantly larger in the combined modality plan than in the single modality proton plan. This does come at the cost of a larger dose to several OARs: in particular, larger volumes of the liver and the stomach

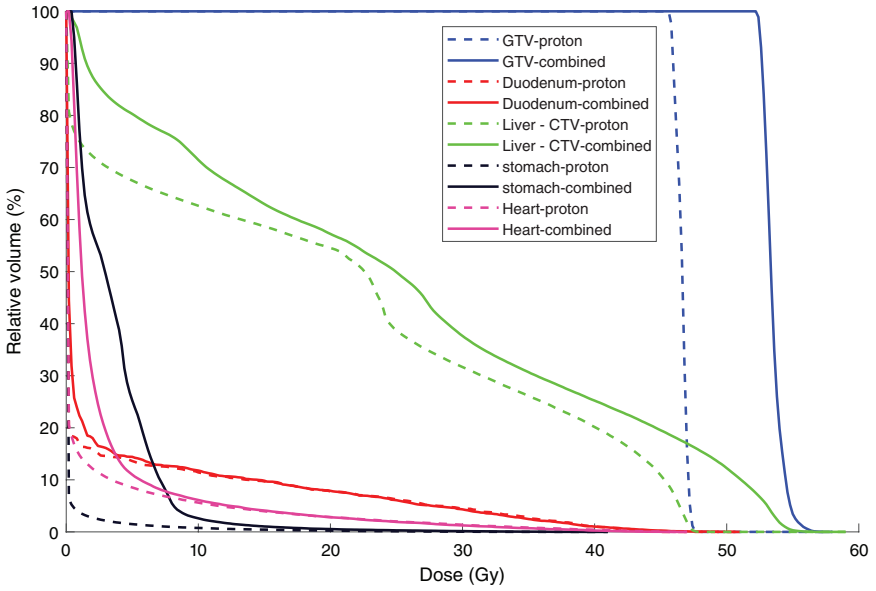

Figure 5. DVH for proton and combined modality plans for patient P_1. Dashed lines are the optimal single modality proton solution, solid lines the optimal combined modality solution. The combined modality solution attains a higher average GTV BED while satisfying all constraints, but at the cost of increased dose to several OARs, most notably the healthy liver.

receive a low to medium dose instead of no dose, due to the photon dose distribution. However, all OAR constraints are naturally still satisfied.

4.2. Demonstration of OAR sparing

From figure 5 it may seem that simply allowing higher OAR doses for a single modality proton plan could yield similarly large tumor BED values as the combined modality plan. This is in general not the case. To show this we performed additional analysis for patient P_1 by minimizing healthy liver BED for both single modality proton and combined proton–photon treatments, subject to the constraint that the tumor BED should be at least 72.5 Gy_{10} (the mean GTV BED value in the optimal combined plan when GTV BED was maximized). All other OAR constraints are omitted. The resulting DVH is displayed in figure 6, where also the optimal combined modality plan is displayed. The resulting proton plan uses 15 fractions of 3.6 Gy. The resulting liver dose distributions are comparable, however by not using proton fractions alone combined modality is better able to spare the duodenum. As given in table 1, at 15 fractions the duodenum volume that receives more than 40 Gy should be at most 0.5*cc*, but as indicated in figure 6 this volume in the proton plan is in fact 1.3*cc*. This result indicates that, even in cases where combined modality is not able to reduce mean liver BED compared to single modality proton treatments (see section 3.1), combined modality plans may still yield benefits in terms of OAR sparing for other OARs than healthy liver.

Moreover, as mentioned in section 3.1, for two patients (P_2 and P_3) combined modality treatment was found to be able to lower healthy liver mean dose. In case of mean tumor BED maximization, for patient P_2 the binding constraint in the single modality proton and photon treatments are the 0.5*cc* small bowel DVH constraint and the mean liver dose constraint, respectively. For P_3, the situation is similar, the only difference being that the binding constraint for single modality proton is the 0.5*cc* stomach DVH constraint. For the mean healthy liver BED minimization, the lower bound on the GTV mean BED is set at the GTV BED of the optimal single modality proton treatment. For these two patients (P_2 and P_3) the single modality proton treatment attains the maximum GTV BED using fewer than the maximum of 15 fractions. Consequently, for the combined modality treatment it is easier to get to this GTV BED, because it can better spare the second OAR (small bowel or stomach) than the single modality proton treatment. Hence, combined treatments can exploit the fractionation effect to a larger extent for sparing OARs. Furthermore, although the photon dose distribution has a higher mean healthy liver dose than the proton dose distribution, the locations of their healthy liver high dose areas need not be the same. Hence, a combined treatment may deliver the healthy liver dose more homogeneously, leading to a lower dose shape factor (Perkó *et al* 2018) and consequently a lower healthy liver BED as well.

4.3. Illustration of group 2

Patient P_6 was also clinically treated with 15 proton fractions. Two CT slices are displayed in figure 7, visualizing the dose distributions for both photons and protons. The relevant organs are the liver, the stomach, and the cord (see figures 7(c) and (d) showing the lower CT slice). The dose tolerances for the healthy liver mean dose

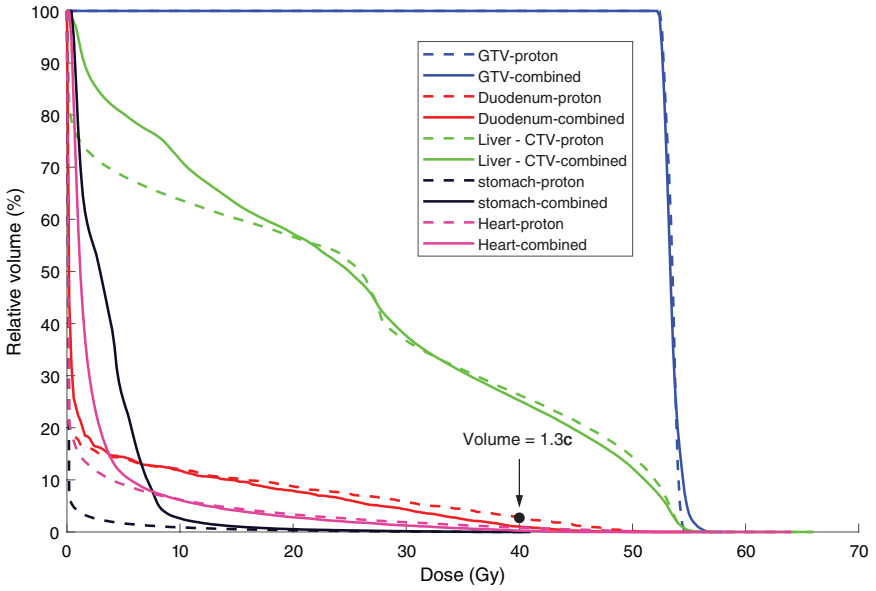

Figure 6. DVH for proton and combined modality plans for patient P_1 for mean liver BED minimization. Mean tumor BED is constrained to be at least 72.5 Gy_{10}. Dashed lines are the optimal single modality proton solution, solid lines the optimal combined modality solution. The healthy liver dose distribution is comparable, while the single modality proton solution violates the duodenum 0.5*cc* DVH constraint.

constraint are 17 Gy in 5 fractions and 27 Gy in 15 fractions, for the other constraints see table 1. The clinical plan violated the 700*cc* constraint, hence it is omitted here as well.

The optimal GTV BED is 92.6 Gy_{10} and is obtained at 15 proton fractions, see column 3 of table 4. The corresponding physical dose to the GTV is 64.7 Gy. There are no combined modality treatments that yield a higher average GTV BED, the reason for this is shown in figure 7. As seen in the CT slices of figures 7(a) and (b), both the proton and the photon high dose region fall almost entirely inside the liver, so the healthy part of the liver gets a large average dose in both modalities. However, the tumor is very close to a small extension of the stomach, and protons spare this part slightly better than photons, making single modality proton treatments optimal.

In the single modality proton plan the binding constraint is the (17 Gy in five fractions) mean dose constraint on the liver, while the 0.5*cc* stomach DVH constraint is almost binding. In the single modality photon plan this is reversed; the stomach constraint is binding, while the liver mean dose constraint is almost binding. Similar to patient P_1, we check the influence of restricting the single modality photon case to constant dose per fraction: the optimal treatment delivers an average GTV BED of 82.7 Gy_{10}, using six fractions of 7.8 Gy fx^{-1}, again a negligible difference (compared to column 1 in table 4).

Using the results reported in table 4, let us compare the optimal single modality proton solution to the combined modality alternative that uses seven proton fractions and eight photon fractions. The average GTV BED of this combined modality solution is 90.1 Gy_{10}, and the corresponding BED equivalent physical GTV dose is 63.3 Gy. This is a decrease of 1.4 Gy in BED equivalent GTV dose for a substitution of eight fractions.

When substituting some proton fractions in the single modality proton treatment with photon fractions, the remaining space in the 0.5*cc* stomach DVH constraint is used as well. This is because protons damage the part of the stomach that is close to the tumor slightly more than photons. Consequently, both the 0.5*cc* stomach DVH constraint and the liver mean dose constraint become binding. However, as protons spare the liver a bit better, the attainable average GTV BED decreases. The BED to the cord also increases significantly compared to the single modality proton plan, where it received almost no dose. Nevertheless, the tolerance level of the 0.5*cc* cord DVH constraint is not violated.

Figure 8 shows the DVH graph for the GTV, healthy liver, stomach, cord and duodenum, in terms of BED equivalent dose. The dashed lines are the optimal single modality proton plan which uses 15 proton fractions, and the solid lines are the alternative combined modality plan which uses seven proton fractions and eight photon fractions. We see that indeed the BED equivalent average GTV dose is slightly higher for the single modality proton plan than for the combined modality plan. Furthermore, the low dose volumes for the liver, stomach and cord increase. At the same time, the high dose volume for the liver decreases.

4.4. Connection to clinically used NTCP models

In the Netherlands a model based approach is used to determine proton therapy eligibility (Blanchard *et al* 2016, Widder *et al* 2016, Bijman *et al* 2017). Patients are eligible for protons if normal tissue complication probability

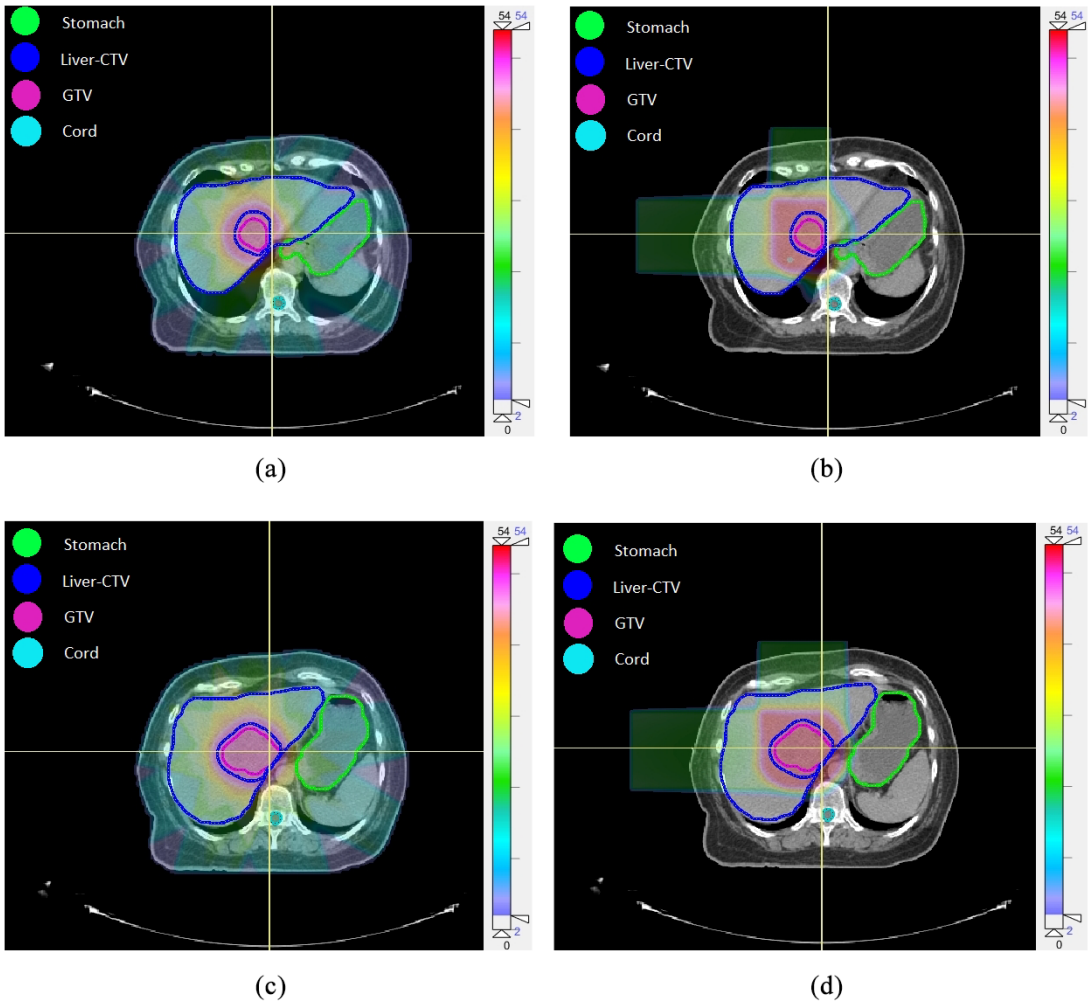

Figure 7. Spatial dose distribution in photon and proton plans of patient P_6 in two slices. The GTV, liver-CTV, stomach and cord are delineated. CT slice 1 is the higher of the two slices. (a) Photon, CT slice 1. (b) Proton, CT slice 1. (c) Photon, CT slice 2. (d) Proton, CT slice 2.

Table 4. Results for patient P_6. The reported combined modality treatment is an alternative to the single modality proton treatment. It delivers a slightly lower BED equivalent dose to the GTV, but uses fewer proton fractions.

	Single modality photon	Single modality proton	Combined modality
GTV BED	82.8 Gy_{10}	92.6 Gy_{10}	90.1 Gy_{10}
BED equivalent dose	59.3 Gy	64.7 Gy	63.3 Gy
Photon fractions	5 fx (8.7 Gy fx^{-1})	—	8 fx (3.7 Gy fx^{-1})
	1 fx (1.0 Gy fx^{-1})		
Proton fractions	—	15 fx (4.3 Gy fx^{-1})	7 fx (4.8 Gy fx^{-1})

(NTCP) models show that protons offer a significant improvement over photons. As NTCP models are often BED distribution based models (Perkó *et al* 2018), our work fits this procedure nicely. Our approach can show that when using a combined modality approach we can get a higher tumor BED for the same BED constraint, or alternatively for a given tumor dose we can decrease OAR BED. This takes the current Dutch approach to the next level, not only making binary decisions between photons or protons, but instead looking into the correct combination of proton and photon fractions for complication minimization.

4.5. Clinical aspects and limitations

We do not have a precise measure of the robustness of the combined proton–photon plans that are obtained via the approach of section 2.2. However, any combined proton–photon plan that is obtained via our approach is essentially a weighted average of the input clinical proton and photon plans. As discussed in section 2.2.7 and Perkó *et al* (2018), for all used plans proper clinical measures were taken to handle uncertainties. Therefore, as in any fraction either (a scaled version of) the proton or photon plan is delivered, the combined proton–photon treatment is also robust against the same uncertainties.

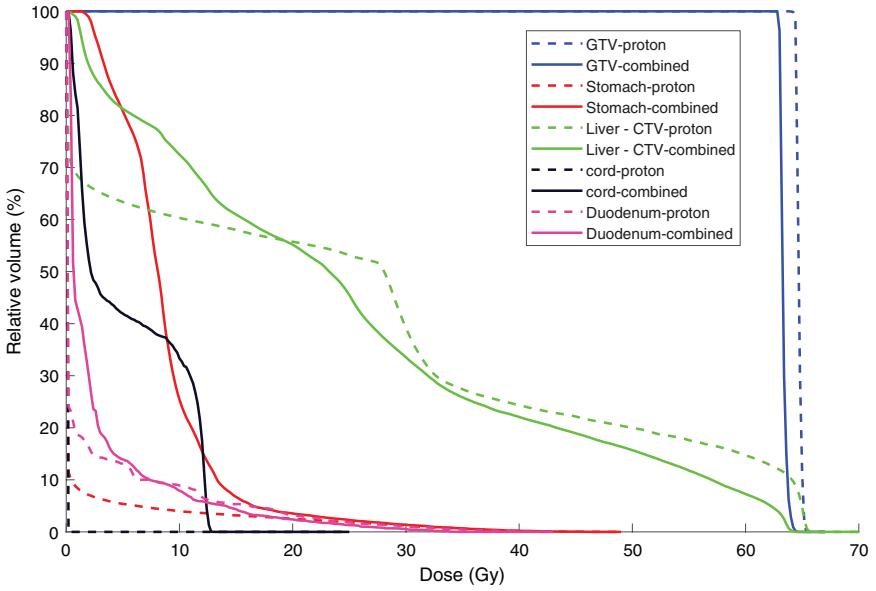

Figure 8. DVH for proton and combined modality plans for patient P_6. The dashed lines are the optimal single modality proton solution, the solid lines are the alternative combined modality solution. The combined modality solution yields a slightly lower average GTV BED, while using eight fewer proton fractions.

As the approach of section 2.2 takes the proton and photon dose distribution as an input, whether or not combined modality is optimal for a patient depends on these initial proton and photon plans. As such, different plans may yield different results. The proton and photon plans used in the numerical study in section 3 were however either clinically used plans, or plans that were derived under clinical circumstances, as if they were to be delivered. This implies that under the same clinical circumstances, our results are representative of the realistic clinical benefit of combined modality treatments.

Our approach excludes spatiotemporal optimization, and simply scales the given proton and photon dose distributions. Since in spatiotemporal optimization of a combined proton–photon treatment the individual dose spatial distributions are also optimized, this may improve on our methodology. However, the results from spatiotemporal optimization can only yield a larger benefit for combined modality treatments compared to what is presented in section 3. That is, the presented results for individual patients should be seen as a 'lower bound' on the benefit of a combined modality treatment for the patient, reinforcing our main conclusions. Furthermore, although spatiotemporal optimization may yield better results, the presented approach has some practical advantages. Planning, reviewing and quality assurance (QA) procedures are well established for single modality treatment plans and these could be seamlessly used for our combined modality approach, as either modality can be separately dealt with. In fact, this is exactly how currently combined treatments are used in the clinic (e.g. in case of a proton machine breakdown when patients are redirected to photon treatments for the remainder of their treatment).

We have only tested our approach on liver patients, thus we cannot make any statements about the potential of combined proton–photon treatment schemes in other tumor sites. Nevertheless, the mathematical approach of section 2.2 does not make any assumptions on the specific tumor site, and is applicable to any case where both a proton and photon dose distribution are available. The reasons why combined modality may be optimal, as demonstrated in section 2.1, can also occur in other tumor sites, particularly those where there are multiple OARs in proximity to the tumor.

In our numerical experiments the objective is to maximize the mean BED to the GTV (a general recommendation for liver patients is to not expand the GTV to a larger CTV (Dawson *et al* 2012)). However, we also performed experiments with maximizing mean CTV BED, indicating that the difference in results from maximizing mean GTV BED is very little. The protocol (Dawson *et al* 2012) also recommends the mean liver dose to be calculated on the liver-GTV, whereas we considered liver-CTV (volume that is healthy with high likelihood). This difference is not expected to influence results either (as the CTV-GTV volume receives very similar doses from both protons and photons).

While our main focus was on tumor BED maximization, we also show that minimizing OAR BED can lead to optimal combined modality treatments for the same reasons. First, appendix A.3 discusses the simplistic analytical model to reveal why also for OAR dose sparing combined modality may be of use. Second, the numerical experiments show that for the patients in group 1 (section 3.1), the combined modality treatment may also achieve lower healthy liver BED. Section 4.2 details these numerical results and additionally shows an example of lower duodenum dose due to difference in spatial dose distribution.

5. Conclusion

Proton therapy has several advantages over conventional photon therapy. However, in current clinical practice protons are not better for all organs in all cases, especially not when larger margins are needed for large motion uncertainty. Consequently, this work analyzed the benefit of combined modality treatments. It is demonstrated both via theoretical results and real patient case studies that combined modality treatments can result in superior dosimetric treatment plan quality. One reason for this is that in case of multiple constraints, one constraint may be more restrictive for one treatment modality, while the other is more restrictive for the other. A second reason is that even in situations where the proton plan is superior in terms of physical dose, using photon fractions can result in treatment plans that are better, due to the fractionation effect.

Results from the case study on real data from patients treated at Massachusetts General Hospital show that for 5 out of 17 patients indeed combined modality treatments outperform the single modality proton treatment, with improvements of up to 14.8% in BED equivalent physical dose. For these patients in our cohort the single modality photon and proton treatments have different binding constraints, while their combination is binding in the optimal combined modality solution, corresponding well with theoretical results.

For several other patients combined modality treatments are near-optimal while using fewer proton fractions. Especially because of the price tag and the limited availability of proton fractions, such alternatives that put less pressure on the proton machine of a certain treatment facility may be very interesting. In conclusion, the potential for combined modality treatments is considerable.

Acknowledgments

The authors thank Ted Hong and John Wolfgang (Massachusetts General Hospital and Harvard Medical School) for their valuable input during discussions.

Appendix A. Mathematical derivation of optimality of combined modality treatments

This section discusses the simplified geometry of figure 1 in section 2.1, and formulates several mathematical models that demonstrate the benefit of combining photons with protons instead of using only protons. The optimization is based on the BED model, which is introduced in section 2, and in section 2.1 the setting is described. For this demonstration we make two assumptions. Note that these assumptions are strictly only made for this analytical exercise highlighting why combined modality can be optimal, and not for the general methodology or any of the real patient cases in the paper.

Assumption A.1. *The protons dose distribution has a larger high dose but smaller low dose region than the photon dose distribution.*

Assumption A.2. *For a fixed tumor dose, the proton dose distribution delivers lower mean dose to OAR 1 than the photon dose distribution.*

Parameters f_i^H and f_i^L denote the high and low dose volume fraction of OAR 1 for modality i, respectively, where $i = \gamma$ denotes photons and $i = p$ denotes protons. Let w denote the high dose volume fraction of OAR 2 for the proton beam. Assumption A.1 mathematically implies that $f_\gamma^H < f_p^H$ and $f_\gamma^L > f_p^L$. Let D_γ^T, the mean tumor dose for photons, and D_p^T, the mean tumor dose for protons, be the decision variables (superscript T refers to the tumor). For the OARs, the low dose can be expressed as $D_i^{\text{low}} = s_i D_i^T$, where $s_i \in [0, 1]$ is the dose sparing factor of modality i for the low dose region. The high dose areas are assumed to receive the full tumor dose, so $D_i^{\text{high}} = D_i^T$. The mean dose in OAR 1 due to modality i can be written as a function of mean tumor dose due to modality i:

$$D_i^{\text{OAR1}}(D_i^T) = s_i f_i^L D_i^T + f_i^H D_i^T = (s_i f_i^L + f_i^H) D_i^T. \tag{A.1}$$

Assumption A.2 implies that for a fixed tumor dose the mean proton dose to OAR 1 is smaller than the mean photon dose to OAR 1, i.e. $s_\gamma f_\gamma^L + f_\gamma^H > s_p f_p^L + f_p^H$. For notational convenience, we introduce the parameters

$$r_\gamma = s_\gamma f_\gamma^L + f_\gamma^H, \; q_\gamma = s_\gamma^2 f_\gamma^L + f_\gamma^H, \tag{A.2a}$$

$$r_p = s_p f_p^L + f_p^H, \; q_p = s_p^2 f_p^L + f_p^H, \tag{A.2b}$$

which provide a linear and quadratic mapping from tumor dose to OAR dose. Using this notation, assumption A.2 implies $r_\gamma > r_p$.

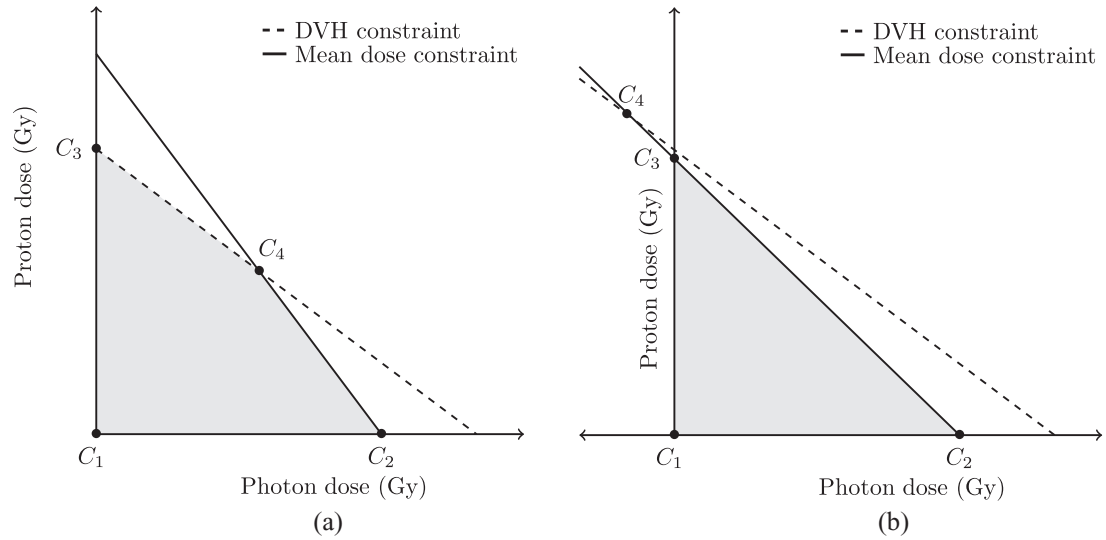

Figure A1. Feasible region (grey) of (A.3), which is the convex hull of (some of) the vertices C_1–C_4. The feasible region is constrained by a DVH constraint (on OAR2) and a mean dose constraint (on OAR1). (a) Feasible region (in grey) for (A.3) if vertex C_4 is feasible. (b) Feasible region (in grey) for (A.3) if vertex C_4 is infeasible because the horizontal coordinate is negative.

The first model (related to section 2.1.1) does not take into account fractionation, and sets a mean dose constraint on OAR 1 and a DVH constraint on OAR 2. In the second model (related to section 2.1.2) we allow for a fractionation effect in OAR 1 but not in the tumor, and we set a mean BED constraint on OAR 1 (OAR 2 is not taken into account). In the supplementary material (section C, suppl.) a third model is discussed, which is an extension of the second model also allowing for fractionation effects in the tumor. In appendix A.3 we take an alternative approach, and minimize OAR BED subject to a prescribed tumor dose.

A.1. Reason 1—mathematical model

To maximize the dose delivered to the tumor, while satisfying all constraints set on the OARs, we rescale the dose distributions, increasing or decreasing the dose in the OARs and the tumor simultaneously. That is, D_γ^T and D_p^T are the decision variables.

We set a mean dose constraint on OAR 1 and a DVH constraint on OAR 2. Let $D_{\text{mean}}^{\text{tol}}$ denote the largest average dose that OAR 1 can tolerate, as determined by the physician. Suppose the DVH constraint states that no more than a fraction k of the volume of OAR 2 may receive a higher dose than $D_{\text{dvh}}^{\text{tol}}$. This constraint can potentially be more restrictive for the proton dose distribution than for the photon dose distribution. In the photon plan OAR 2 receives only low dose. If $k < w$, the total dose to the proton high dose volume w must not exceed the tolerance level $D_{\text{dvh}}^{\text{tol}}$. OAR 2 receives only photon low dose. Therefore, volume w receives a dose of $s_\gamma D_\gamma^T + D_p^T$ in the combined modality plan, which must be below the DVH tolerance dose $D_{\text{dvh}}^{\text{tol}}$. The optimization problem with both a mean dose constraint and a DVH constraint reads

$$\max_{D_\gamma^T,\, D_p^T} \; D_\gamma^T + D_p^T \tag{A.3a}$$

$$\text{s.t.} \qquad r_\gamma D_\gamma^T + r_p D_p^T \leqslant D_{\text{mean}}^{\text{tol}} \tag{A.3b}$$

$$s_\gamma D_\gamma^T + D_p^T \leqslant D_{\text{dvh}}^{\text{tol}} \tag{A.3c}$$

$$D_\gamma^T \geqslant 0, \;\; D_p^T \geqslant 0. \tag{A.3d}$$

In the problem described by (A.3) it does not necessarily have to hold that using only photons or only protons is optimal. Problem (A.3) is a linear programming problem with two variables. The feasible region of (A.3b) is illustrated in figure A1. It can easily be verified that the vertices of the feasible region are

$$C_1 = \Big(0, 0\Big), \qquad C_2 = \Big(\min\Big\{\frac{D_{\text{mean}}^{\text{tol}}}{r_\gamma}, \; \frac{D_{\text{dvh}}^{\text{tol}}}{s_\gamma}\Big\}, 0\Big),$$

$$C_3 = \Big(0, \min\Big\{\frac{D_{\text{mean}}^{\text{tol}}}{r_p}, \; D_{\text{dvh}}^{\text{tol}}\Big\}\Big), \qquad C_4 = \Big(\frac{D_{\text{mean}}^{\text{tol}} - D_{\text{dvh}}^{\text{tol}} r_p}{r_\gamma - s_\gamma r_p}, \; \frac{r_\gamma D_{\text{dvh}}^{\text{tol}} - s_\gamma D_{\text{mean}}^{\text{tol}}}{r_\gamma - s_\gamma r_p}\Big).$$

Linear programming theory states that the optimal solution is attained in one (or more) of these vertices. Vertex C_1 is clearly not optimal because the corresponding objective value is 0. Vertices C_2 and C_3 comprise single modality solutions and C_4 is the combined modality solution. Vertex C_4 is only a feasible vertex if both coordinates are positive. It readily follows that this leads to the following condition:

$$r_p < \frac{D^{\text{tol}}_{\text{mean}}}{D^{\text{tol}}_{\text{dvh}}} < \frac{r_\gamma}{s_\gamma}. \tag{A.4}$$

In figure A1(a) this condition holds, so all vertices C_1, C_2, C_3 and C_4 are feasible. In figure A1(b) condition (A.4) does not hold, and the horizontal coordinate of C_4 is negative. In this situation, the mean dose constraint (A.3*b*) is binding at any feasible vertex. In case the vertical coordinate of C_4 is negative, DVH constraint (A.3*c*) is binding at any feasible vertex.

We are interested in conditions under which C_4 is optimal, in case it is feasible (the situation in figure A1(a)), rather than the single modality solutions (vertices C_2 and C_3). In (A.3*a*) the coefficients for D_1^T and D_2^T are both 1, so the objective function is a straight line with slope -1. Due to assumption A.2 the mean dose to OAR 1 is lower for the proton dose distribution than for the photon dose distribution. Therefore, in the mean dose constraint (A.3*b*) the coefficient for proton dose is smaller than that for photon dose, implying that the slope for the mean dose constraint is smaller than -1. If the slope of the DVH constraint (A.3*c*) is larger than -1, combined modality is optimal. This reduces to $s_\gamma < 1$, which holds by definition. Hence, combined modality is always optimal as long as the solution candidate C_4 is feasible, which holds if the dose tolerances satisfy condition (A.4).

For example, let $f_\gamma^L = 0.82$, $f_\gamma^H = 0.18$, $s_\gamma = 0.32$ be the parameters for the photon dose distribution, and let $f_p^L = 0.37$, $f_p^H = 0.23$ and $s_p = 0.38$ be the parameters for the proton dose distribution. Then the proton high dose area is larger than the photon high dose area, while the photon mean dose to OAR 1 is larger than the proton mean dose to OAR 1. Condition (A.4) reads

$$0.37 < \frac{D^{\text{tol}}_{\text{mean}}}{D^{\text{tol}}_{\text{dvh}}} < 1.38, \tag{A.5}$$

which is satisfied by for example $D^{\text{tol}}_{\text{mean}} = 20$ Gy and $D^{\text{tol}}_{\text{dvh}} = 35$ Gy.

A.2. Reason 2—mathematical model

We extend the previous model to allow for a fractionation effect in OAR 1. For this model, OAR 2 is ignored to demonstrate that even with a single OAR combined modality treatments can be optimal. Let ρ denote the inverse α/β-ratio of OAR 1. With r_i and q_i defined by (A.2*a*), one can verify that the mean BED to OAR 1 due to modality i is

$$\text{BED}_i^{\text{OAR1}}(d_i, N_i) = r_i \sum_{t_i=1}^{N_i} d_{i,t_i} + \rho q_i \sum_{t_i=1}^{N_i} d_{i,t_i}^2. \tag{A.6}$$

We assume that the α/β-ratio in the tumor is very large so that we can neglect the fractionation effect in the tumor. That is, we are interested in the physical tumor dose

$$D^T = D_\gamma^T + D_p^T = \sum_{t_\gamma=1}^{N_\gamma} d_{\gamma,t_\gamma} + \sum_{t_p=1}^{N_p} d_{p,t_p}. \tag{A.7}$$

We aim to maximize the total tumor dose while constraining mean OAR BED below a fixed value BED_{tol}. The optimization problem looks as follows:

$$\max_{d_\gamma,\, d_p} \ \sum_{t_\gamma=1}^{N_\gamma} d_{\gamma,t_\gamma} + \sum_{t_p=1}^{N_p} d_{p,t_p}, \tag{A.8a}$$

$$\text{s.t.} \quad r_\gamma \sum_{t_\gamma=1}^{N_\gamma} d_{\gamma,t_\gamma} + \rho q_\gamma \sum_{t_\gamma=1}^{N_\gamma} d_{\gamma,t_\gamma}^2 + r_p \sum_{t_p=1}^{N_p} d_{p,t_p} + \rho q_p \sum_{t_p=1}^{N_p} d_{p,t_p}^2 \leqslant \text{BED}_{\text{tol}}, \tag{A.8b}$$

$$d_{\gamma,t_\gamma} \geqslant 0, \ t_\gamma = 1, \ldots, N_\gamma, \ d_{p,t_p} \geqslant 0, \ t_p = 1, \ldots, N_p. \tag{A.8c}$$

Our decision variables are $d_\gamma \in \mathbb{R}_+^{N_\gamma}$ and $d_p \in \mathbb{R}_+^{N_p}$. In (A.8*a*), N_γ and N_p are considered fixed parameters, and treatment plans with fewer than N_γ photon or N_p proton fractions can be found by setting the corresponding elements of d_γ and d_p at zero. In other words, N_γ and N_p are parameters indicating an upper bound on the number of photon and proton fractions, respectively.

In the supplementary material (section D, suppl.) it is shown that the following problem is equivalent to (A.8*a*):

$$\max_{x_\gamma,\, y_\gamma,\, x_p,\, y_p} \quad x_\gamma + x_p, \tag{A.9a}$$

$$\text{s.t.} \quad r_\gamma x_\gamma + \rho q_\gamma y_\gamma + r_p x_p + \rho q_p y_p \leqslant \text{BED}_{\text{tol}}, \tag{A.9b}$$

$$\sqrt{y_\gamma} \leqslant x_\gamma \leqslant \sqrt{N_1 y_\gamma}, \tag{A.9c}$$

$$\sqrt{y_p} \leqslant x_p \leqslant \sqrt{N_2 y_p}, \tag{A.9d}$$

$$x_\gamma \geqslant 0,\ y_\gamma \geqslant 0,\ x_p \geqslant 0,\ y_p \geqslant 0. \tag{A.9e}$$

For a fixed dose to (part of) the OAR, the BED to (that part of) the OAR will be lower if this dose is administered over multiple fractions. Because in this problem the number of fractions does not influence the damage to the tumor (fractionation in the tumor is ignored), the optimal solution will always use the maximum number of allowed fractions. Therefore, it will always hold that $x_\gamma = \sqrt{N_\gamma y_\gamma}$ and $x_p = \sqrt{N_p y_p}$. Plugging this in (A.9*b*) gives an optimization problem with only decision variables x_γ and x_p. Furthermore, at optimality (A.9*b*) will hold with equality, because the total physical dose to the tumor is increased until the OAR BED tolerance is reached. Therefore, we can rewrite (A.9*b*) in terms of x_γ and eliminate variable x_p as well.

The resulting optimization problem reads

$$\max_{x_p} \quad f(x_p) \tag{A.10a}$$

$$\text{s.t.} \quad 0 \leqslant x_p \leqslant x_p^U, \tag{A.10b}$$

where

$$f(x_p) = x_p + \frac{N_\gamma}{2\rho q_\gamma}\Big(- r_\gamma + \big(r_\gamma^2 - 4\frac{\rho q_\gamma}{N_\gamma}(r_p z + \frac{\rho q_p}{N_p}x_p^2 - \text{BED}_{\text{tol}})\big)^{\frac{1}{2}}\Big) \tag{A.11a}$$

$$x_p^U = \frac{N_p}{2\rho q_p}\Big(- r_p + \big(r_p^2 + 4\frac{\rho q_p}{N_p}\text{BED}_{\text{tol}}\big)^{\frac{1}{2}}\Big). \tag{A.11b}$$

Function $f(x_p)$ is concave, because it is a composite function of a nondecreasing concave function and a concave function (Boyd and Vandenberghe 2004). Hence, it follows that a single modality photon treatment is optimal if $f'(0) \leqslant 0$, a single modality proton treatment is optimal if $f'(x_p^U) \geqslant 0$, and combined modality is optimal otherwise. The derivative of the objective function is

$$f'(x_p) = 1 + \big(- r_p - 2\frac{\rho q_p}{N_p}x_p\big)\Big(4\frac{\rho q_\gamma}{N_\gamma}(\text{BED}_{\text{tol}} - x_p(r_p + \frac{\rho q_p}{N_p}x_p)) + r_\gamma^2\Big)^{-\frac{1}{2}}. \tag{A.12}$$

From (A.12) the following easily follows:

- Single modality photon is never optimal;
- Combined modality is optimal if $\text{BED}_{\text{tol}} > \dfrac{N_p(r_\gamma^2 - r_p^2)}{4\rho q_p}$; (A.13)
- Single modality proton is optimal otherwise.

Using basic algebra the optimal dose per fraction values can be calculated for both situations. As concluded in section 2.1.2 there is a threshold for BED_{tol} beyond which the benefit of fractionation outweighs the worse OAR sparing properties of the photons in terms of physical dose.

A.3. Minimization of OAR BED

To show that the optimality of combined modality treatments is not restricted to the previously presented models, we analyse a model where we do not maximize tumor dose but minimize OAR BED, while delivering a prescribed dose $\hat{D}$ to the tumor. We immediately apply the mapping from tumor dose to OAR dose defined by (A.2*a*), and the reformulation provided in the supplementary material (section D, suppl.). The optimization problem looks as follows:

$$\min_{x_\gamma,\, y_\gamma,\, x_p,\, y_p} \quad r_\gamma x_\gamma + \rho q_\gamma y_\gamma + r_p x_p + \rho q_p y_p, \tag{A.14a}$$

$$\text{s.t.} \quad x_\gamma + x_p = \hat{D}, \tag{A.14b}$$

$$\sqrt{y_\gamma} \leqslant x_\gamma \leqslant \sqrt{N_\gamma y_\gamma}, \tag{A.14c}$$

$$\sqrt{y_p} \leqslant x_p \leqslant \sqrt{N_p y_p}, \tag{A.14d}$$

$$x_\gamma \geqslant 0,\ y_\gamma \geqslant 0,\ x_p \geqslant 0,\ y_p \geqslant 0. \tag{A.14e}$$

Similar to appendix A.2 the optimal solution will always use the maximum number of allowed fractions. Therefore, it will always hold that $x_\gamma = \sqrt{N_\gamma y_\gamma}$ and $x_p = \sqrt{N_p y_p}$. This leads to a problem with four variables and three equality constraints, which can be simplified to a problem with one variable. Making the substitution $z = \sqrt{y_p}$ leads to

$$\min_z \ \big(\rho q_\gamma \frac{N_\gamma}{N_p} + \rho q_p\big) z^2 + \Big((r_p - r_\gamma)\sqrt{N_p} - 2\rho q_\gamma \hat{D}\frac{\sqrt{N_p}}{N_\gamma}\Big) z + \big(p_\gamma \hat{D} + \rho \frac{q_\gamma}{N_\gamma}\hat{D}^2\big), \tag{A.15a}$$

$$\text{s.t.} \quad 0 \leqslant x_p \leqslant \frac{\hat{D}}{\sqrt{N_p}}. \tag{A.15b}$$

The first order condition, i.e. zero-derivative, gives

$$\hat{z} = \frac{(r_\gamma - r_p)N_\gamma\sqrt{N_p} + 2\rho q_\gamma \sqrt{N_p}\hat{D}}{2\rho(q_p N_\gamma + q_\gamma N_p)}.$$

Because $r_\gamma > r_p$, it holds that $\hat{z} > 0$, so a single modality solution using only photons cannot be optimal. It is easily verified that $\hat{z}$ satisfies (A.15*b*) if $\hat{D} \geqslant D^*$, where

$$D^* = \frac{(r_\gamma - r_p)N_p}{2q_p\rho}. \tag{A.16}$$

In this case, we can write $x_\gamma = \hat{D} - x_p = \hat{D} - \sqrt{N_p}\hat{z}$, from which it follows that if $\hat{D} > D^*$ holds we have $x_\gamma > 0$ (and thus $y_\gamma > 0$). This implies a combined proton-photon fractionation scheme. On the other hand, if $\hat{D} \leqslant D^*$, then the optimal solution to (A.15*a*) is

$$x_p = \frac{\hat{D}}{\sqrt{N_p}}.$$

Because $\sqrt{y_p} = x_p$, we obtain $x_p = \hat{D}$, $x_\gamma = 0$ and $y_\gamma = 0$. Summarizing, we find that two situations can be distinguished with regard to a single modality or combined modality solution:

$$\begin{cases} \hat{D} \leqslant D^* & \text{A single modality solution using only protons is optimal.} \\ \hat{D} > D^* & \text{A combined modality solution is optimal.} \end{cases} \tag{A.17}$$

Using basic algebra the optimal dose per fraction values can be calculated for both situations. Similar to appendix A.2, combined modality is optimal if a threshold is exceeded, although there the threshold is in terms of OAR BED tolerance while here it is in terms of the prescribed tumor dose. Nevertheless, the intuition for the current result is analogous to the intuition for the result in appendix A.2, which is presented in section 2.1.2.

Appendix B. Single modality optimal fractionation problem

Let ρ^T be the inverse α/β ratio for the tumor, let $\mathcal{M}$ denote the set of constraints and let ρ^m denote the inverse α/β ratio for constraint $m \in \mathcal{M}$. In Saberian *et al* (2015) it is shown that the single modality optimal fractionation problem with maximum point dose constraints, DVH constraints and mean dose constraints can be formulated as

$$\max_{x,\ y} \ rx + \rho^T q y \tag{B.1a}$$

$$\text{s.t.} \quad \sigma^m x + \rho^m (\sigma^m)^2 y \leqslant B^m,\ \forall m \in \mathcal{M} \tag{B.1b}$$

$$y \leqslant \gamma^* x \tag{B.1c}$$

$$c^* x \leqslant y \tag{B.1d}$$

$$x \geqslant 0,\ y \geqslant 0, \tag{B.1e}$$

where r, q, and σ^m, B^m, $\forall m$, are parameters. Furthermore,

$$\gamma^* = \min_{m\in\mathcal{M}} \frac{-1+\sqrt{1+4\rho^m B^m}}{2\sigma^m\rho^m} \tag{B.2a}$$

$$c^* = \min_{m\in\mathcal{M}} \frac{-1+\sqrt{1+4\rho^m B^m/N}}{2\sigma^m\rho^m}, \tag{B.2b}$$

where N is the maximum allowed number of fractions. Variables x and y denote the dose and sum of squared doses. Problem (B.1a) is a two-variable linear programming problem and is easily solved.

ORCID iDs

S C M ten Eikelder https://orcid.org/0000-0001-7883-8506
T Bortfeld https://orcid.org/0000-0002-3883-0398
Z Perkó https://orcid.org/0000-0002-0975-4226

References

Audet C and Dennis J E Jr 2003 Analysis of generalized pattern searches *SIAM J. Optim.* **13** 889–903
Badri H, Watanabe Y and Leder K 2016 Optimal radiotherapy dose schedules under parametric uncertainty *Phys. Med. Biol.* **61** 338–64
Bertuzzi A, Bruni C, Papa F and Sinisgalli C 2013 Optimal solution for a cancer radiotherapy problem *J. Math. Biol.* **66** 311–49
Bijman R G *et al* 2017 Impact of model and dose uncertainty on model-based selection of oropharyngeal cancer patients for proton therapy *Acta Oncol.* **56** 1444–50
Blanchard P *et al* 2016 Toward a model-based patient selection strategy for proton therapy: external validation of photon-derived normal tissue complication probability models in a head and neck proton therapy cohort *Radiother. Oncol.* **121** 381–6
Bodey R, Evans P and Flux G 2004 Application of the linear-quadratic model to combined modality radiotherapy *Int. J. Radiat. Oncol. Biol. Phys.* **59** 228–41
Bortfeld T, Ramakrishnan J, Tsitsiklis J and Unkelbach J 2015 Optimization of radiation therapy fractionation schedules in the presence of tumor repopulation *INFORMS J. Comput.* **27** 788–803
Boyd S and Vandenberghe L 2004 *Convex Optimization* (Cambridge: Cambridge University Press)
Dawson L A *et al* 2012 RTOG 1112: Randomized Phase III study of sorafenib versus stereotactic body radiation therapy followed by sorafenib in hepatocellular carcinoma *Technical Report* (Philadelphia, PA: Radiation Therapy Oncology Group)
Deasy J, Blanco A and Clark V 2003 CERR: a computational environment for radiotherapy research *Med. Phys.* **30** 979–85
Fowler J 1989 The linear-quadratic formula and progress in fractionated radiotherapy *Br. J. Radiol.* **62** 679–94
Fowler J 2010 21 years of biologically effective dose *Br. J. Radiol.* **83** 554–68
Kim M, Stewart R and Philips M 2015 A feasibility study: selection of a personalized radiotherapy fractionation schedule using spatiotemporal optimization *Med. Phys.* **42** 6671–8
Mizuta M, Takao S, Date H, Kishimoto N, Sutherland K, Onimaru R and Shirato H 2012 A mathematical study to select fractionation regimen based on physical dose distribution and the linear-quadratic model *Int. J. Radiat. Oncol. Biol. Phys.* **84** 829–33
Nill S 2001 Development and application of a multi-modality inverse treatment planning system *PhD Thesis* University of Heidelberg
Nourollahi S, Ghate A and Kim M 2018 Optimal modality selection in external beam radiotherapy *Math. Med. Biol.* dqy013
O'Connor D, Yu V, Nguyen D, Ruan D and Sheng K 2018 Fraction-variant beam orientation optimization for non-coplanar IMRT *Phys. Med. Biol.* **63** 045015
Perkó Z, Bortfeld T, Hong T, Wolfgang J and Unkelbach J 2016 Optimal fractionation schemes for liver SBRT based on BED *18th Int. Conf. on the Use of Computers in Radiation Therapy*
Perkó Z, Bortfeld T, Hong T, Wolfgang J and Unkelbach J 2018 Derivation of mean dose tolerances for new fractionation schemes and treatment modalities *Phys. Med. Biol.* **63** 035038
Saberian F, Ghate A and Kim M 2015 A two-variable linear program solves the standard linear-quadratic formulation of the fractionation problem in cancer radiotherapy *Oper. Res. Lett.* **43** 254–8
Saberian F, Ghate A and Kim M 2016 Optimal fractionation in radiotherapy with multiple normal tissues *Math. Med. Biol.* **33** 211–52
Saberian F, Ghate A and Kim M 2017 Spatiotemporally optimal fractionation in radiotherapy *INFORMS J. Comput.* **29** 422–37
Unkelbach J and Papp D 2015 The emergence of nonuniform spatiotemporal fractionation schemes within the standard BED model *Med. Phys.* **42** 2234–41
Unkelbach J, Bangert M, Bernstein K, Andratschke N and Guckenberger M 2018 Optimization of combined proton–photon treatments *Radiother. Oncol.* **128** 133–8
Unkelbach J, Craft D, Salari E, Ramakrishnan J and Bortfeld T 2013a The dependence of optimal fractionation schemes on the spatial dose distribution *Phys. Med. Biol.* **58** 159–67
Unkelbach J, Zeng C and Engelsman M 2013 Simultaneous optimization of dose distributions and fractionation schemes in particle radiotherapy *Med. Phys.* **40** 091702
Wein L, Cohen J and Wu J 2000 Dynamic optimization of a linear-quadratic model with incomplete repair and volume-dependent sensitivity and repopulation *Int. J. Radiat. Oncol. Biol. Phys.* **47** 1073–83
Widder J *et al* 2016 The quest for evidence for proton therapy: model-based approach and precision medicine *Int. J. Radiat. Oncol. Biol. Phys.* **95** 30–6
Withers H 1985 Biological basis for altered fractionation schemes *Cancer* **55** 2086–95
Yang Y and Xing L 2005 Optimization of radiotherapy dose-time fractionation with consideration of tumor specific biology *Med. Phys.* **32** 3666–77